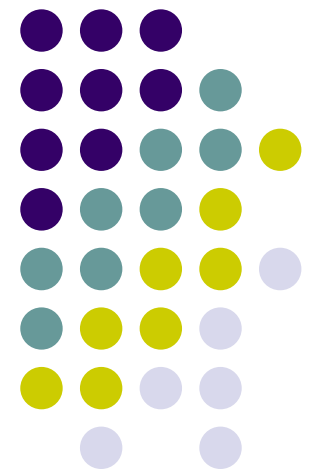




Institut für Theoretische Physik

Universität Würzburg

Correlations between Kondo clouds in nearly AFM Kondo lattices



M.N.Kiselev and K.A.Kikoin

Competition between Kondo and AFM order in heavy fermion compounds

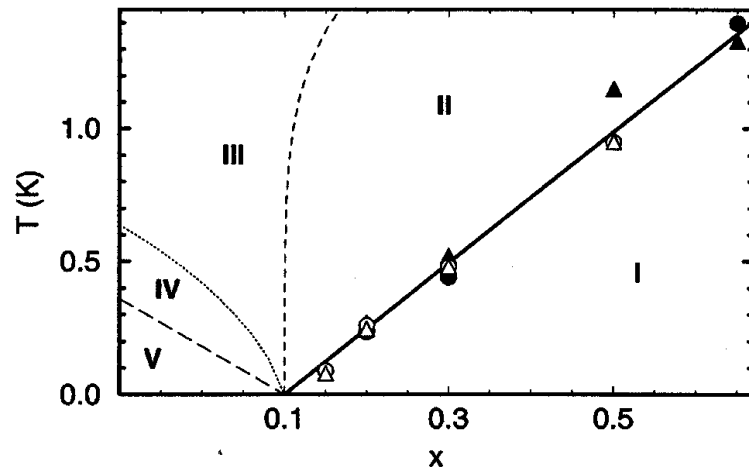


FIG. 1. Phase diagram of $\text{CeCu}_{6-x}\text{Au}_x$. The points are Néel temperatures [7] (open and closed symbols for single and polycrystals, respectively), the solid line denotes the phase transition, the dashed lines are theoretical crossover lines. The regions are described in the text.

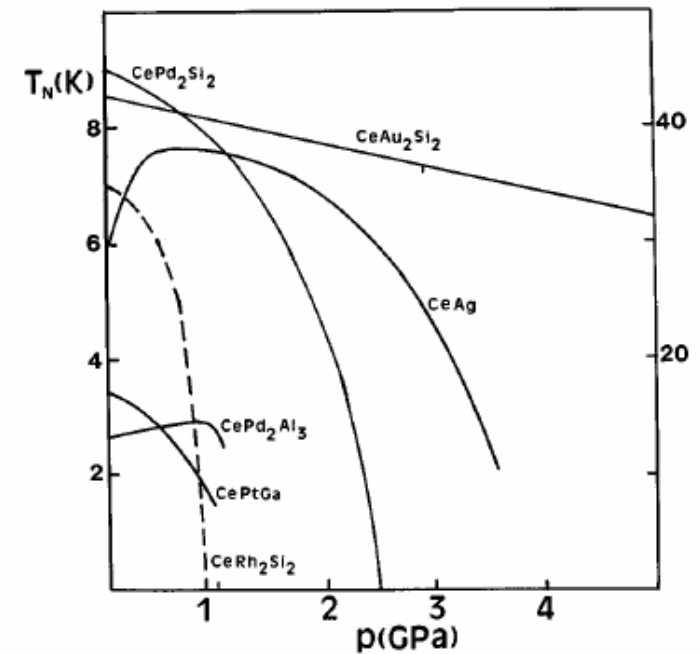


FIG. 2. Experimental curves of the pressure dependence of the Néel temperature for some cerium compounds. The full lines correspond to the left scale for the Néel temperature, while the dotted line of the CeRh_2Si_2 compound corresponds to the right scale.

A.Rosch et al.PRL 79,159 (1997)

Disordered Kondo systems

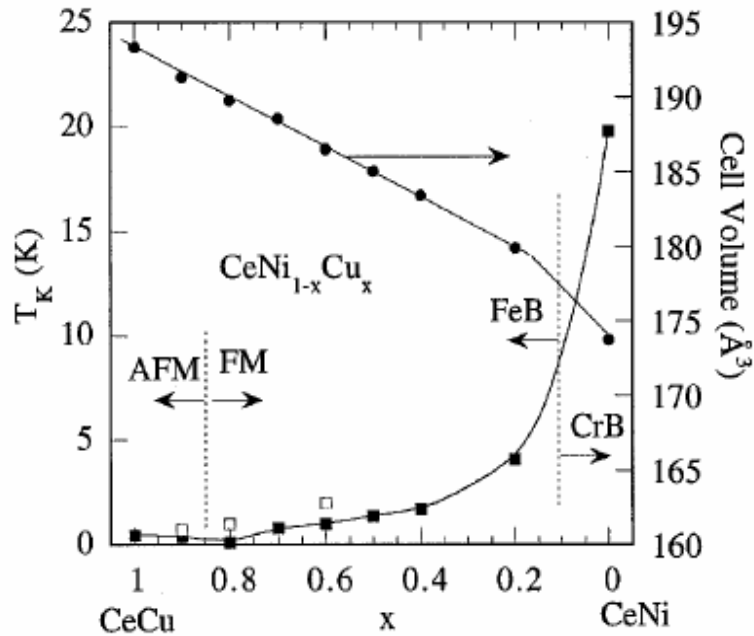


FIG. 1. Concentration dependence of the cell volume (full circles) and the Kondo temperature estimated from different techniques: magnetic susceptibility ($|\theta_p|/10$, full squares), quasielastic neutron scattering (QENS, open squares) for the $\text{CeNi}_{1-x}\text{Cu}_x$ series. The broken lines separate the FeB-CrB crystallographic structures and AFM-FM magnetic states. Full lines are guides for the eyes.

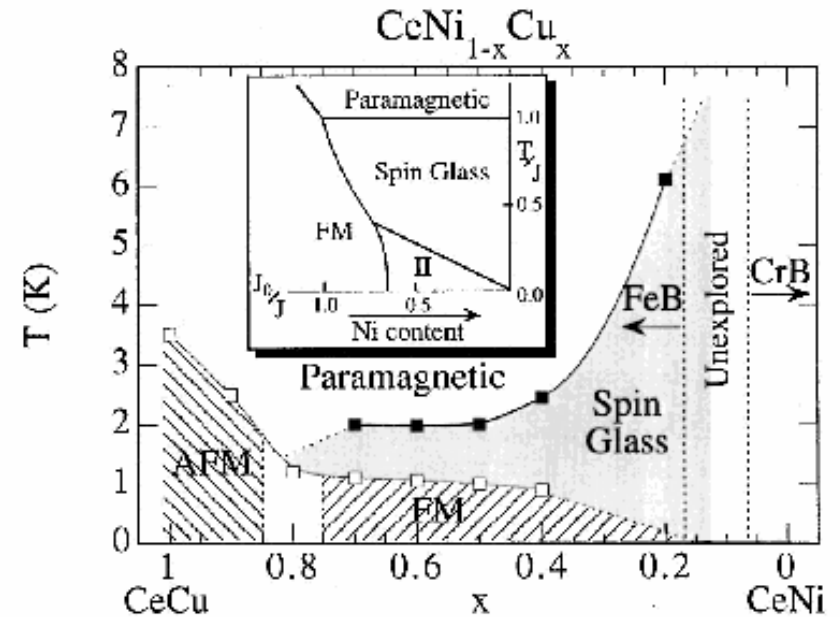
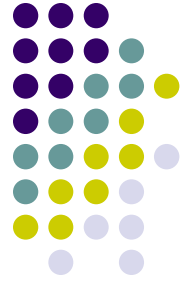


FIG. 4. Magnetic phase diagram for the $\text{CeNi}_{1-x}\text{Cu}_x$ series as a function of Cu concentration, where open squares represent the long-range magnetic ordering temperature $T_{C,N}$ and full squares represent the spin-glass freezing temperature T_f . Inset: Van Hemen classical phase diagram proposed in Ref. 19. The arrow shows the direction of the displacement for increasing Ni content to help the comparison with the experimental diagram.

J.Garcia Soldevilla et al. PRB 61, 6821 (2000)

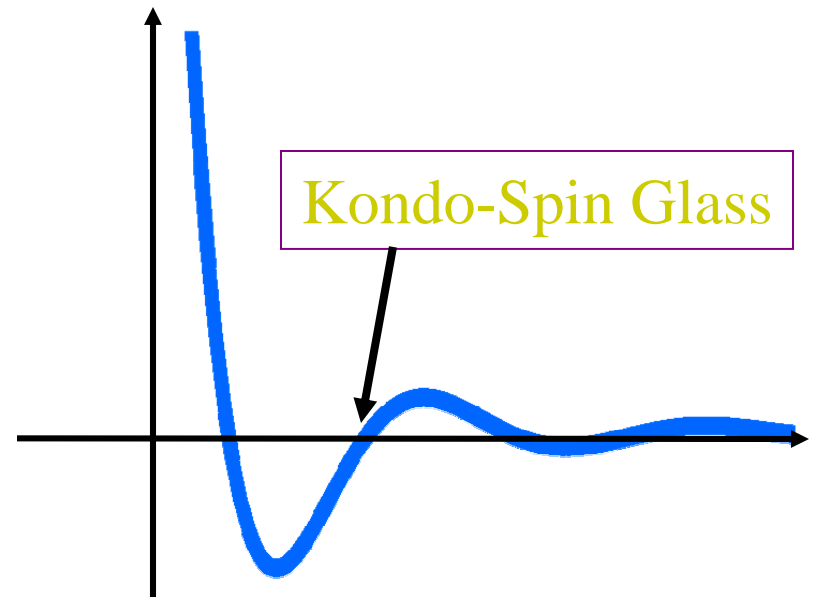
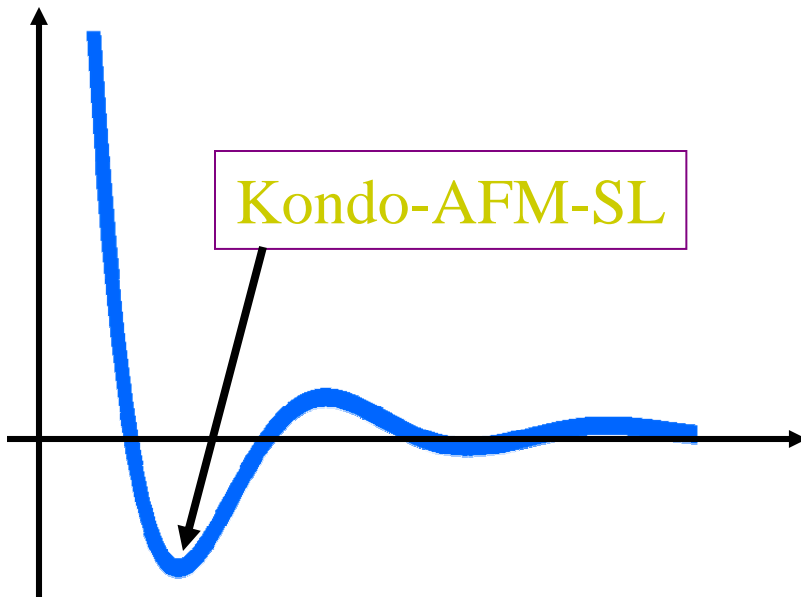
Model



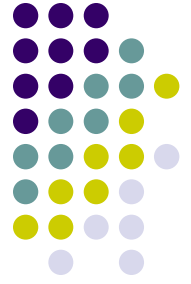
$$H = \sum_k \varepsilon(k) c_{k,\sigma}^+ c_{k,\sigma} + J \sum_i \vec{S}_i \vec{S}_i + \sum_{ij} I_{ij} \vec{S}_i \vec{S}_j$$

d-electrons
Kondo
RKKY

$$I_{ij} = I^{RKKY} = - \left(\frac{J^2}{\varepsilon_F} \right) \frac{\cos \left[2k_F R_{ij} - \pi (d+1) / 2 + \delta(R_{ij}) \right]}{(2k_F R_{ij})^d}$$

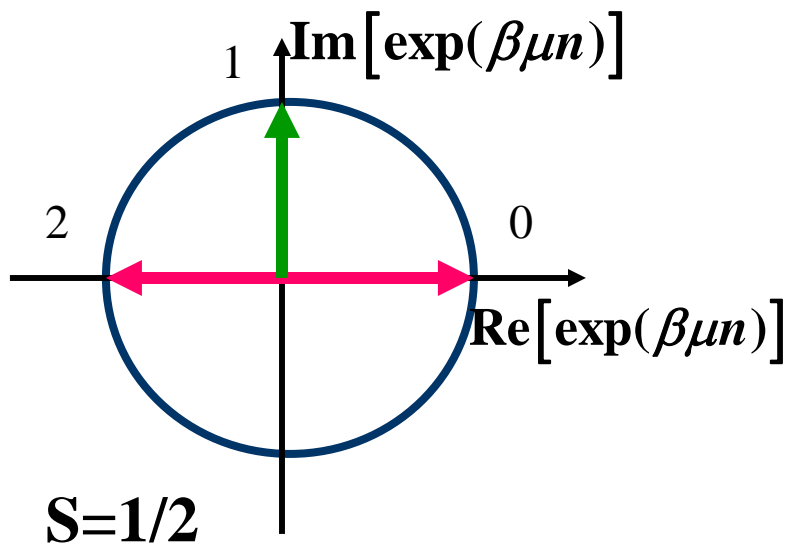


Methods

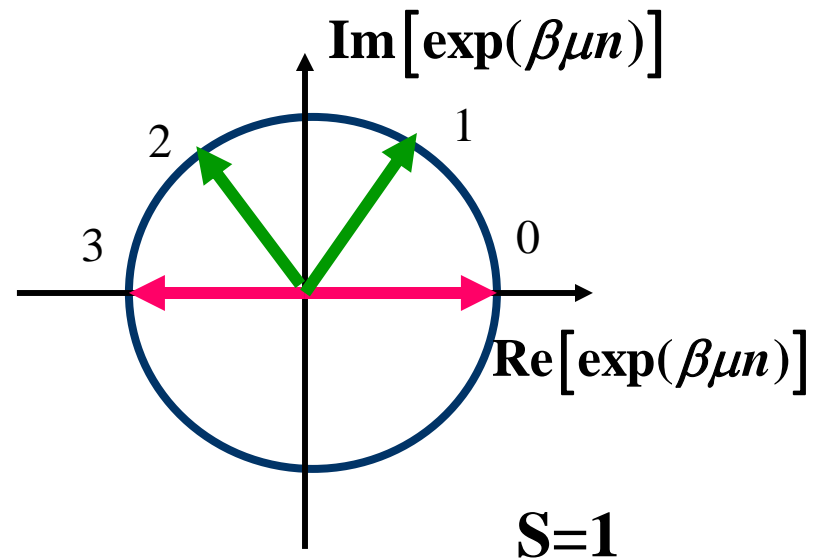


Semi-fermionic representation

$$\vec{S} = f_{\alpha}^{\dagger} \vec{\tau}_{\alpha\beta} f_{\beta}$$



$$\omega = 2\pi T (n + 1/4)$$

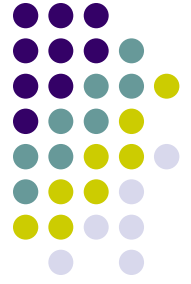


$$\omega = 2\pi T (n + 1/3)$$

$$\mu = -i \frac{\pi T}{2S + 1}$$

$$Z_S = \text{Tr} \left[\exp(-\beta H_S) \right] = A \text{Tr} \left[\exp(-\beta H_F + \beta \mu N_F) \right]$$

Ginzburg-Landau functional for KL model



Program:

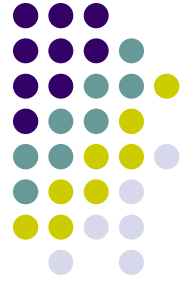
- Represent spins in terms of semi-fermions
- Integrate out the highest energies
- Introduce effective bosonic fields responsible for magnetic (spin glass, spin liquid) correlations
- Introduce effective „semi-bosonic“ fields describing Kondo correlations
- Calculate a free energy taking into account Kondo corrections, construct Ginzburg-Landau functional
- Derive new saddle point equations for magnetic (SL) transitions
- Include fluctuations

$$\beta F_{N,\Delta} = \frac{\beta |I| z N^2}{4} \tau_N + c_N N^4 + \frac{\beta |I| z \Delta^2}{2} + c_{sl} \Delta^4$$

$$\beta F_{SG} = \frac{z(\beta I)^2}{4} q^2 \tau_{SG} - c_{SG} q^3 + d_{SG} q^4$$

Notations: N-Neel, Δ - Spin Liquid, q – Spin Glass, ϕ - Kondo, $\tau_\alpha = 1 - \frac{T_\alpha}{T}$

Antiferromagnetic transition



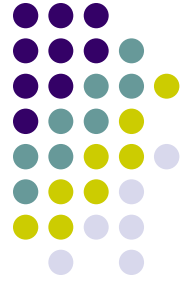
$$A_N = \sum_{q,n} \left[\frac{1}{J} - \Pi(N, q) \right] |\phi(q)|^2 - \text{Tr} \frac{1}{J_\varrho} N_\varrho N_{-\varrho}$$

$$N = \tanh \left(\frac{I_\varrho N}{2T} \right) \left[1 - \frac{a_N}{\ln(T/T_K)} \frac{\cosh^2(I_\varrho N / 2T)}{\cosh^2(I_\varrho N / T)} \right]$$

Local-field corrections reduce the Neel temperature

Kondo screening suppresses AFM transition

RVB spin liquid crossover



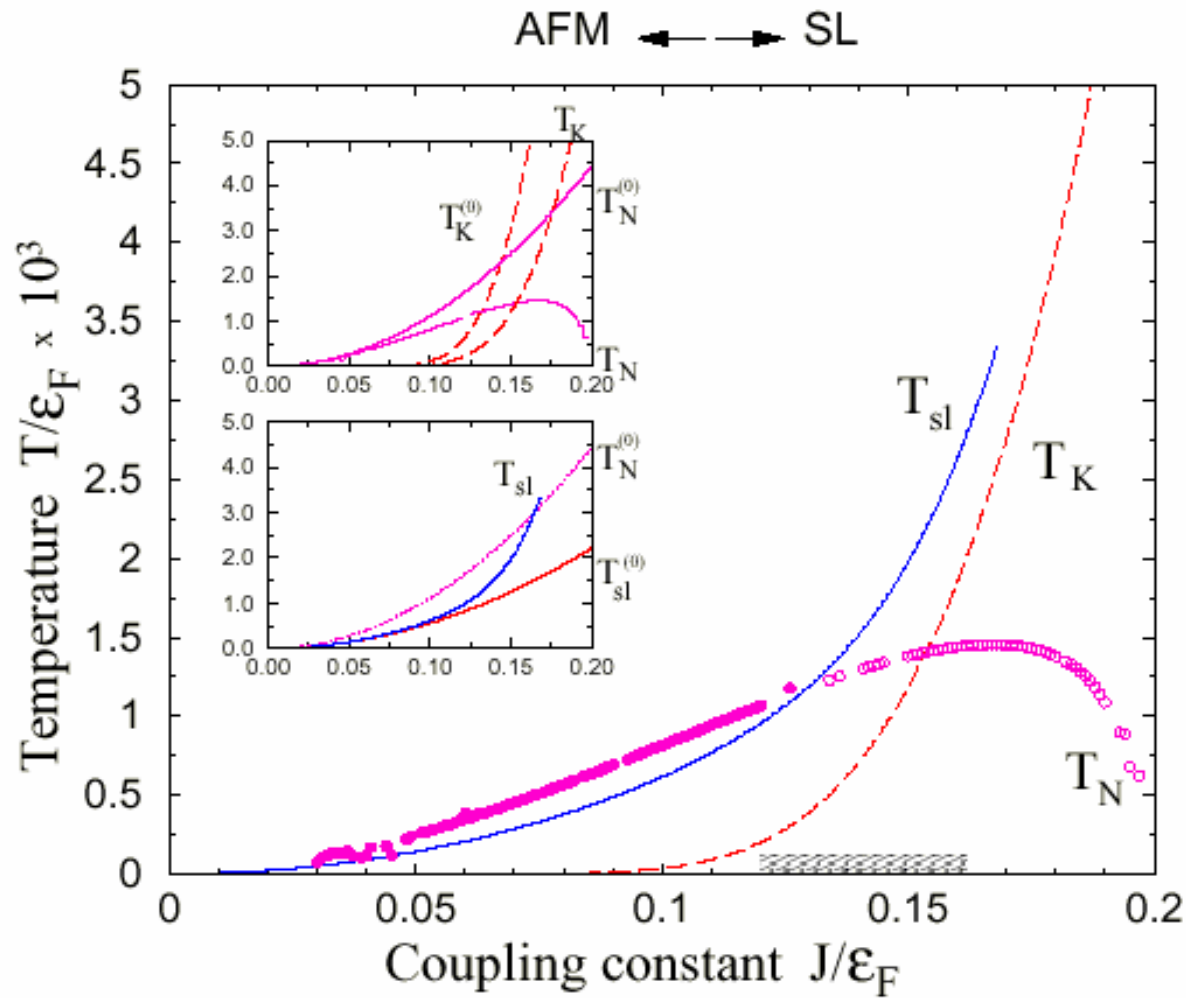
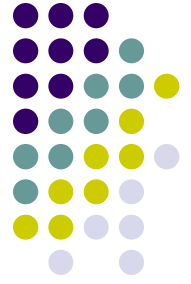
$$A_{\Delta} = \sum_{q,n} \left[\frac{1}{J} - \Pi(\Delta, q) \right] |\phi(q)|^2 - \text{Tr} \frac{1}{J_{p-k}} \Delta_p \Delta_k$$

$$\Delta = \sum_q \nu(q) \left[\tanh \left(\frac{I_q \Delta}{T} \right) + a_{sl} \frac{I_q \Delta}{T \ln(T / T_K)} \right]$$

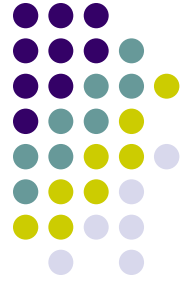
Kondo „antiscreeing“ effectively decreases SL free energy

Kondo scattering favors crossover to SL state

Doniach's diagram revisited



Spin glass transition



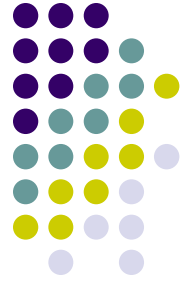
$$\tilde{q} = \int_z^G \tanh^2 \left(\frac{Iz\sqrt{q}/T}{1 + 2c_{sg} (I/T)^2 (\tilde{q} - q) / \ln(T/T_K)} \right)$$

$$q_{EA} = \langle S_i^a(0) S_i^b(t \rightarrow \infty) \rangle \quad q = 1 - \frac{c_{sg}}{\ln(T/T_K)}$$

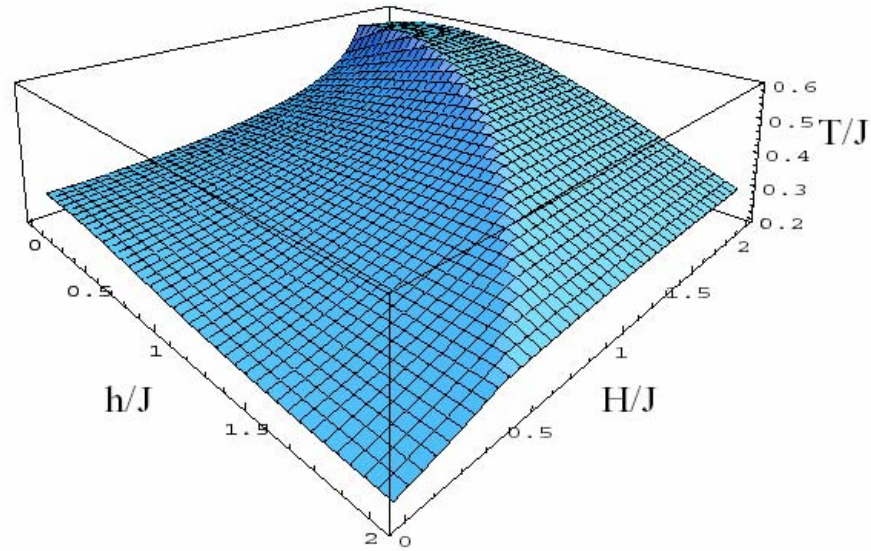
Local correlations reduce the spin-glass transition temperature

Kondo scattering screens Edwards-Anderson order parameter

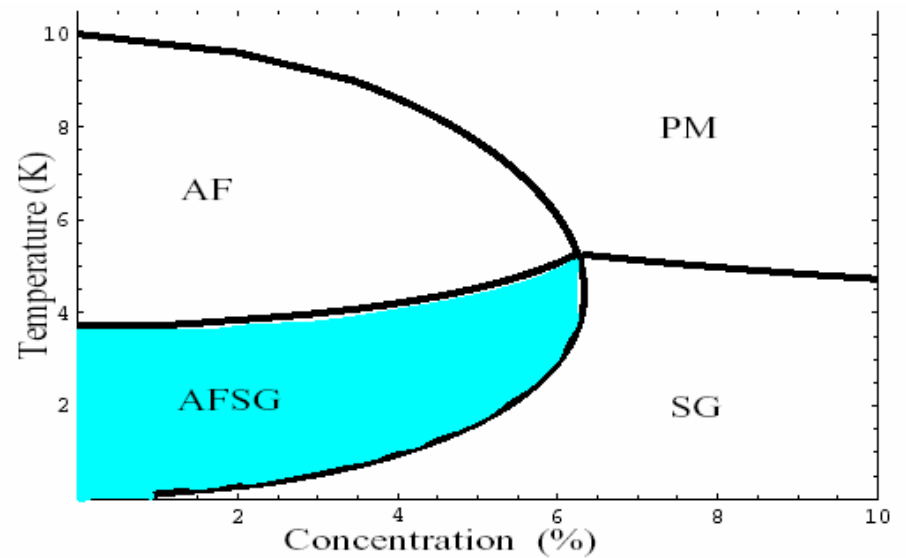
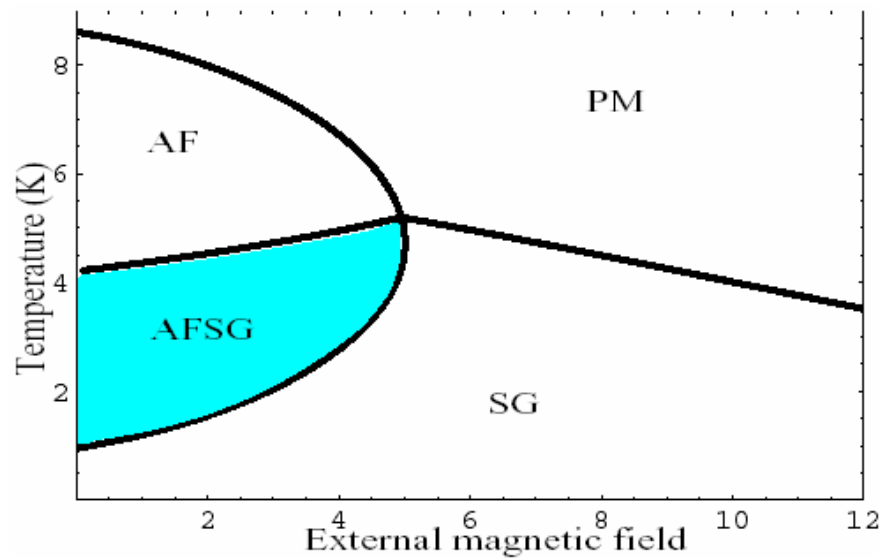
Stability of Replica-symmetric solution



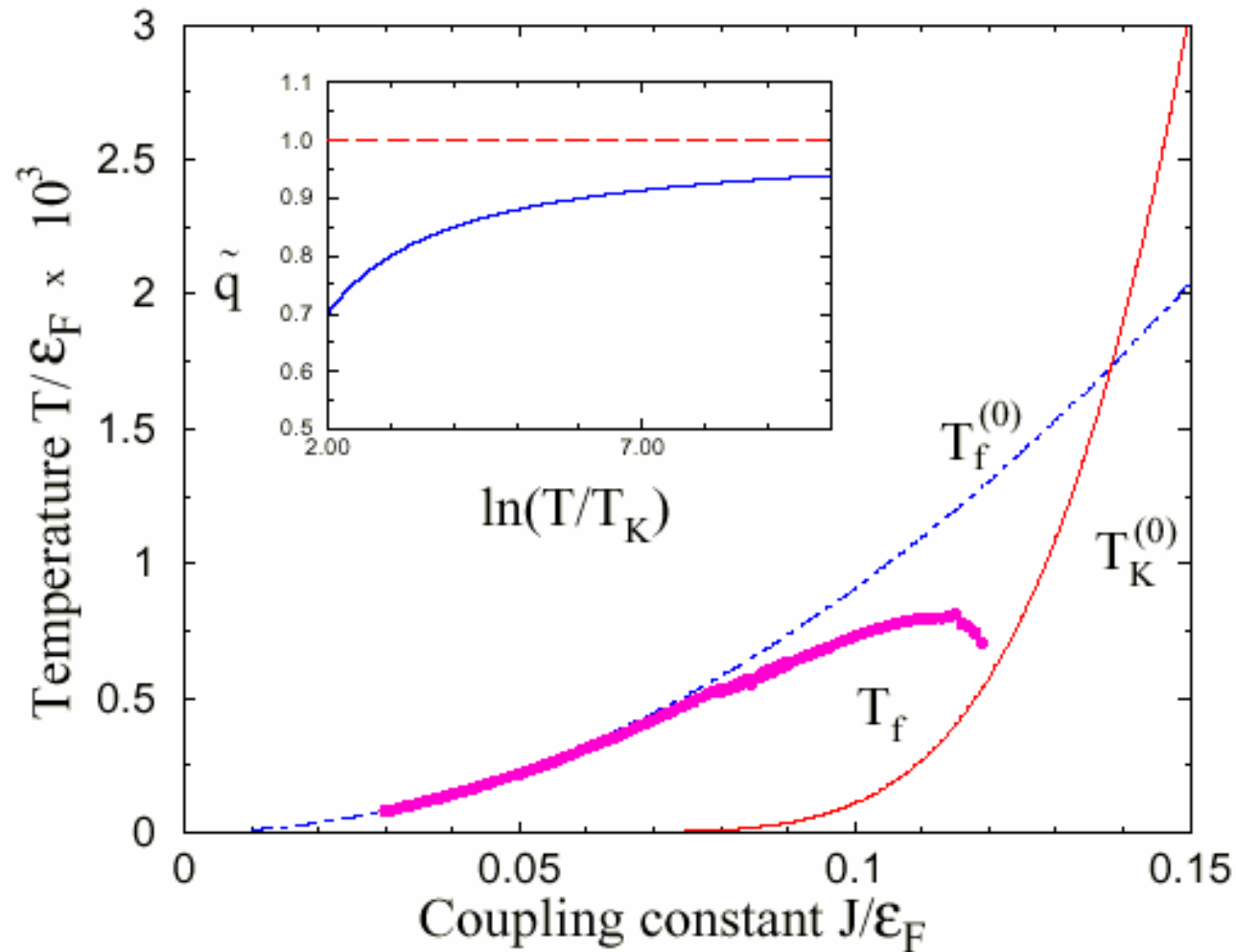
AT-line



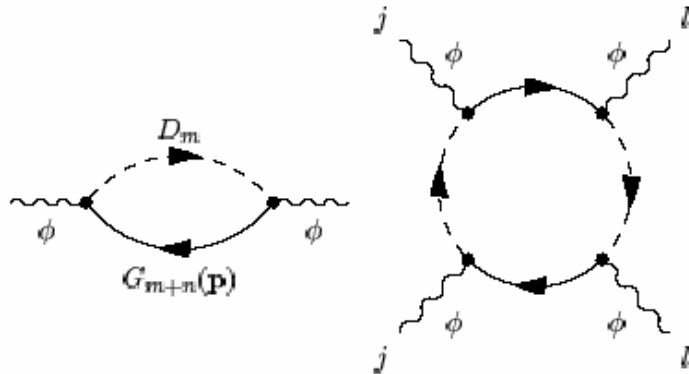
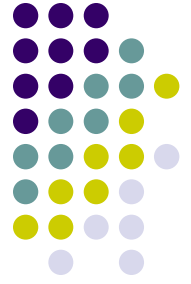
AT-surface



Interplay between Kondo effect and SG transition



Overlap between Kondo Clouds



$$\Pi_4 \sim \frac{1}{T \varepsilon_F^2} \frac{\cos(2k_F R - (d-1)\pi/2)}{(2k_F R)^{d-1}}$$

FIG. 1. Feynman diagrams describing the Kondo cloud (a) and interaction between clouds centered at different sites (b).

$$K(q, \omega) = \langle \phi_{q, \omega} \phi_{q, \omega} \rangle$$

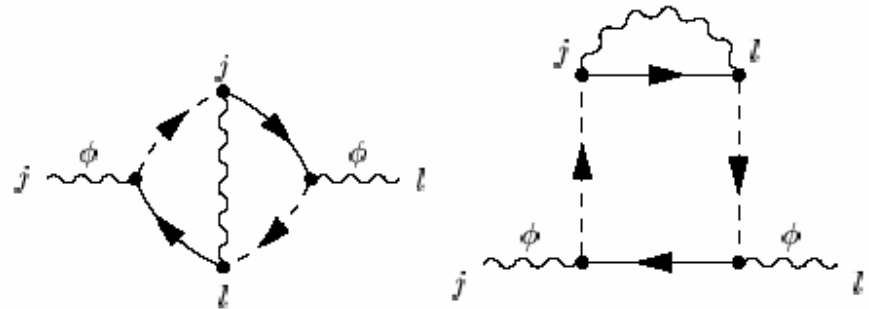
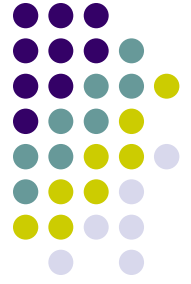


FIG. 2. Feynman diagrams for nonlocal excitations associated with the overlap of Kondo clouds.

Beyond the mean-field



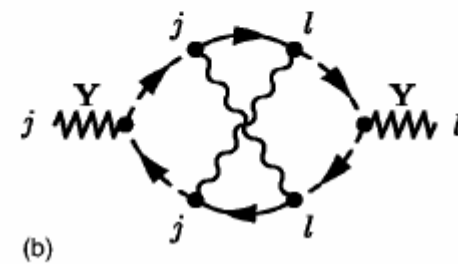
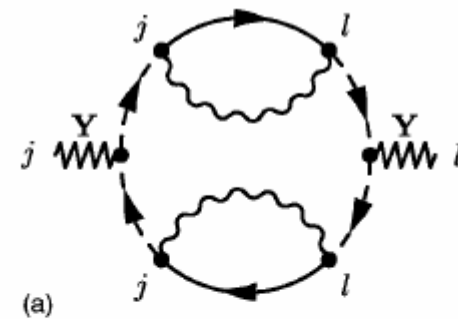
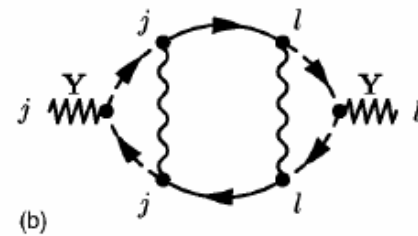
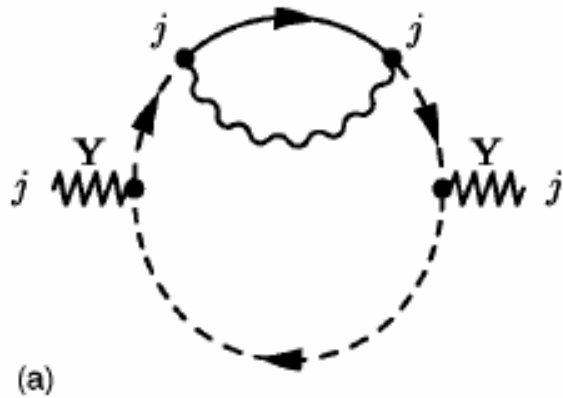
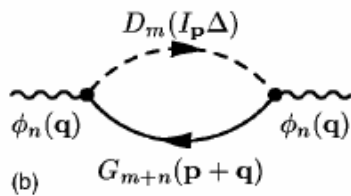
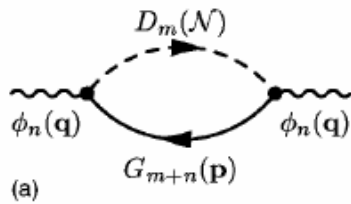
$$K_{loc}^{-1}(\omega) = \frac{-i\omega}{\gamma T} + \ln \left(\frac{\{T, \omega\}}{T_K} \right)$$

$$K^{-1}(q, \omega) = K_{loc}^{-1}(\omega) + \alpha q^2$$

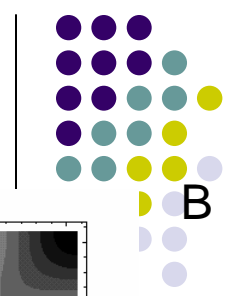
$$\chi^{-1}(T) = \Theta + T^\lambda$$

$\lambda = \lambda(\varepsilon_F, R)$ Critical exponents are non-universal

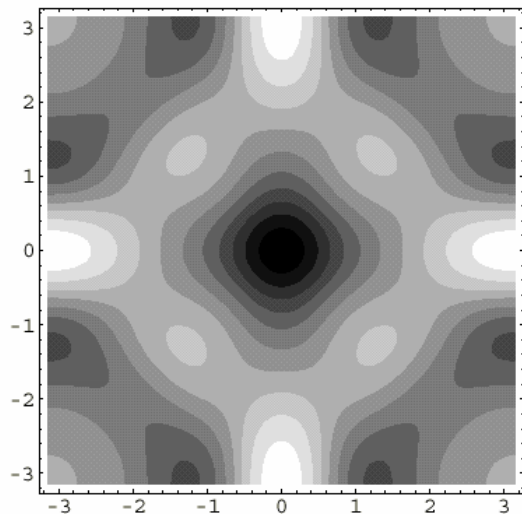
Local and nonlocal corrections to magnetic susceptibility



Correlation between Kondo Clouds

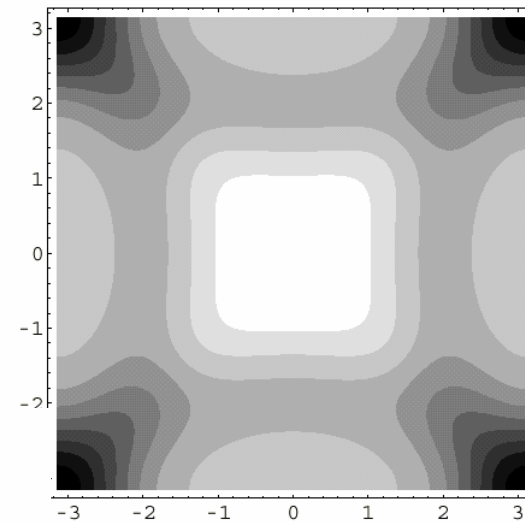


A

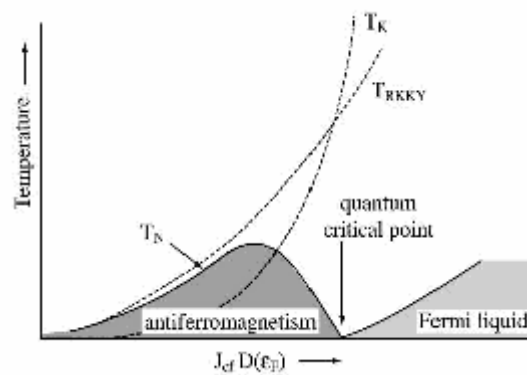


A) $2k_F R = \pi$

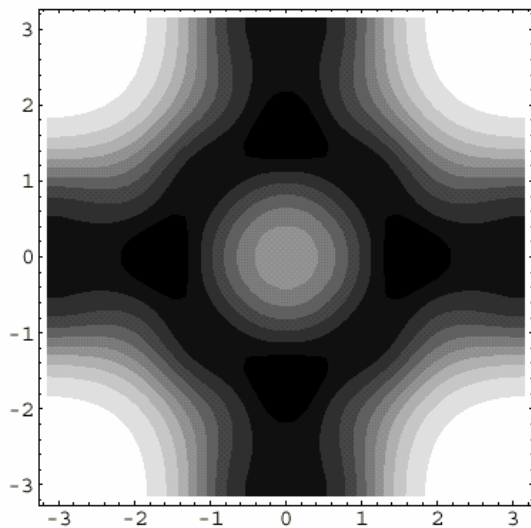
B) $2k_F R = 3\pi / 2$



B

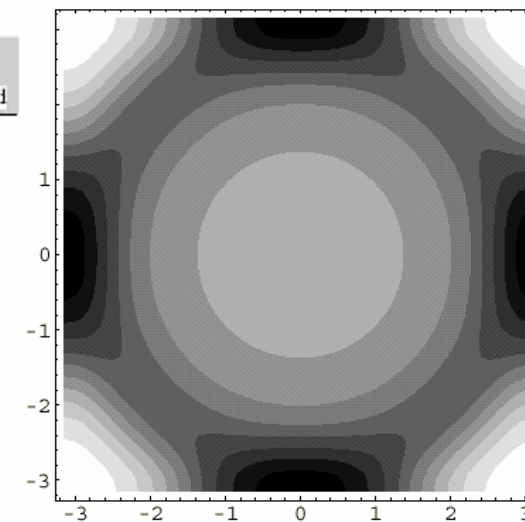


C

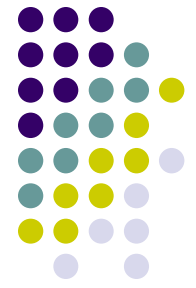


C) $2k_F R = 2\pi$

D) $2k_F R = 5\pi / 2$



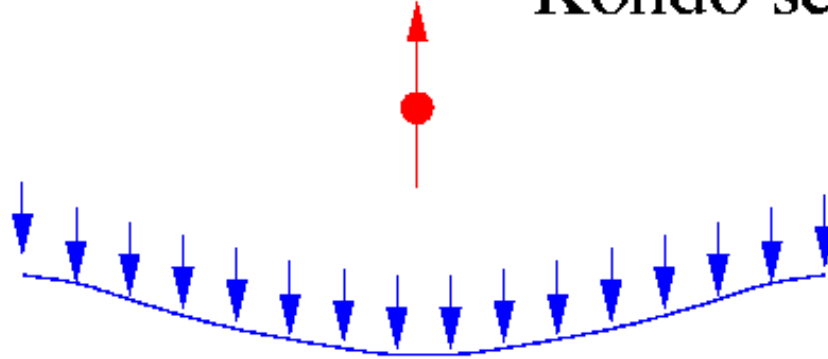
D



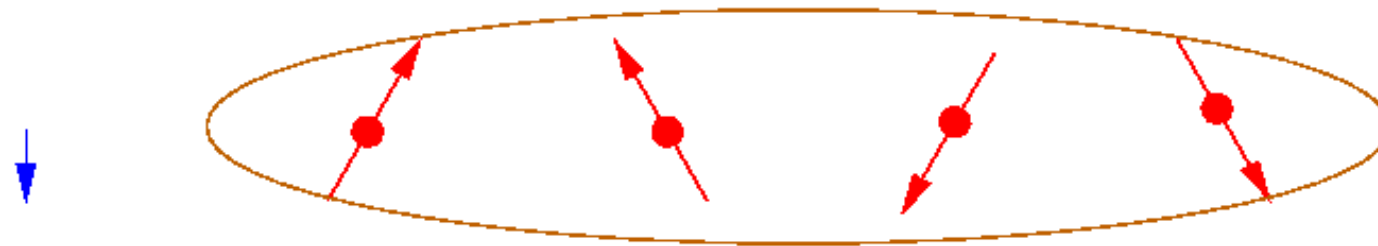
Single impurity Kondo effect

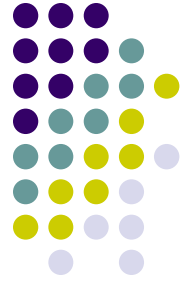


Kondo screening



Short range order





Conclusions

- Kondo screening suppresses magnetic and spin-glass transitions
- Kondo correlations enhance temperature of crossover to spin-liquid state
- Correlations between Kondo clouds result in non-universal temperature dependence of static magnetic susceptibility